Journal of Coastal Research	40	6	1001–1018	Charlotte, North Carolina	November 2024

Analysis of Sandy Beach Morphology Changes and Inundation Events from a High Spatiotemporal Resolution Dataset

Marina Vicens-Miquel[†‡§], Deidre D. Williams[‡], and Philippe E. Tissot[‡§*]

[†]Computer Science Department
Texas A&M University–Corpus Christi
Corpus Christi, TX 78412, U.S.A.

[‡]Conrad Blucher Institute
Texas A&M University–Corpus Christi
Corpus Christi, TX 78412, U.S.A.

[§]NSF AI Institute for Research on Trustworthy AI in Weather, Climate, and Coastal Oceanography (AI2ES)
Norman, OK 73019, U.S.A.

www.cerf-jcr.org

www.JCRonline.org

ABSTRACT

Vicens-Miquel, M.; Williams, D.D., and Tissot, P.E., 2024. Analysis of sandy beach morphology changes and inundation events from a high spatiotemporal resolution dataset. *Journal of Coastal Research,* 40(6), 1001–1018. Charlotte (North Carolina), ISSN 0749-0208.

Coastal inundation creates significant beach management and conservation challenges. The frequency of these events is increasing because of the influence of sea-level rise in combination with background erosion and subsidence in some areas. More accurate predictive models are needed to anticipate potential coastal inundation events for public safety and protection of backshore infrastructure, as well as beach management that can be improved by including the influence of wave runup. Improvement of prediction accuracy requires an in-depth exploration of changes in beach morphology over time and an understanding of the complex interactions responsible for change. This study focuses on changes in beach morphology along a representative beach segment adjacent to Horace Caldwell Pier, Port Aransas, Texas. Ongoing monitoring, initiated in July 2022, provides a rich dataset for analyzing 21 beach-profile surveys, capturing the dynamic evolution of the coastal landscape. Emphasis is placed on quantifying the influence of metocean conditions, particularly high waves with varying periodicity, and wind patterns on morphologic alterations. This research identified two types of inundation events, with two of them resulting in erosion. Consequently, the findings suggest a correlation between the onset of erosion and a maximum dominant wave period of approximately 10 seconds in the study area. The findings contribute to a better understanding of the challenges inherent in predicting coastal inundation and event-based beach morphology changes, fostering informed decision-making that supports sustainable coastal management and developing effective conservation practices.

ADDITIONAL INDEX WORDS: *DEM, beach profile survey, dissipative beach, coastal inundation, shoreline erosion, tidal datums, storm impact.*

INTRODUCTION

Coastal environments are dynamic, and vulnerable landscapes continually shaped by a complex interplay of natural forces (Jackson, Cooper, and del Rio, 2005; Masselink, Kroon, and Davidson-Arnott, 2006; Moser, Jeffress Williams, and Boesch, 2012). The understanding of beach morphology and the factors influencing its evolution are essential for effective coastal management, especially when addressing challenges such as rising relative sea levels and the increase in the frequency of coastal inundation. Despite the value of studying beach dynamics, a notable gap exists in the availability of high-frequency datasets, capturing the changes in beach morphology over time in concert with wave and current measurements and correlated photographic documentation of inundation events.

Historically, beach morphology studies have faced limitations because of inadequate data collection frequency; many of the studies relied on sporadic beach-profile surveys, which have impeded the ability to capture the dynamic nature of the coastal landscapes, often over short periods. Existing datasets, while valuable, often lack the temporal granularity required to discern subtle, but consequential, changes in beach morphology. Furthermore, some studies have attempted to address this limitation by using controlled laboratory environments, such as the large Engineering Research and Development Center (ERDC) laboratory (USACE, 2023a) and the O.H. Hinsdale Wave Research Laboratory (Oregon State University, 2023). The ERDC has conducted research on coastal sediment transport processes (Hamilton *et al.*, 2001), providing valuable insights into the intricate mechanisms shaping coastal environments. Conversely, the O.H. Hinsdale Wave Research Laboratory's focus encompasses coastal and nearshore processing, exploring wave-structure interactions, neahydrodynamics, sediment transport, and the complexities of tsunamis and coastal hazards (Oregon State University, 2023).

One noteworthy study revealed a proportional relationship between the significant wave height of breaking waves and the resulting runup distance on the beach (Roberts, Wang, and Kraus, 2010). This finding is relevant for the present research, offering invaluable guidance about the potential reach of water on the beach during wave events; with forecasted and observed wave characteristics, it serves as an early warning system for potential erosion in these areas. This relationship offers a predictive framework, allowing for anticipation of the extent of wave impact based on the height and period of the breaking waves, thereby enhancing the

DOI: 10.2112/JCOASTRES-D-24-00007.1 received 24 January 2024; accepted in revision 1 July 2024; corrected proofs received 23 July 2024; published pre-print online 12 August 2024.
*Corresponding author: philippe.tissot@tamucc.edu

ability to forecast and be ready to mitigate potential erosion risks more effectively. Moreover, by delving into the specifics of this relationship, it was possible to gain an understanding of the coastal dynamics at play, shedding light on the intricate mechanisms that shape the runup distance. This level of detail is necessary for refining coastal management strategies, ensuring that the predictive models consider the frequency and intensity of wave events and the interplay between wave characteristics and resulting beach dynamics.

Similar studies have been undertaken at the U.S. Army Corps of Engineers (USACE) field facility in Duck, North Carolina, providing valuable data on beach morphology changes under different conditions (USACE, 2023a). The regular monitoring of Duck's nearshore system provides less controlled but more realistic insights from repeated field experiments and further contributes to the understanding of coastal dynamics. Although coastal morphology studies have been conducted in various countries, both in the field and in laboratories, the frequency of high-resolution, real-time observations remains limited, particularly when coupled with real-time video documentation to capture the extent of runup and inundation in the field. Despite the valuable insights gained from high-frequency experiments in the laboratory, it is necessary to acknowledge that the controlled nature of such settings might not fully represent the intricacies of real-world coastal dynamics. The challenge lies in contributing to bridging the gap between the controlled laboratory environment and the complexity of natural coastal systems.

Recognizing these limitations, this research seeks to address the gap in current knowledge by introducing a unique dataset focused on the morphological changes adjacent to Horace Caldwell Pier in Port Aransas, Texas. This dataset, initiated in July 2022, stands as a rare contribution to the field of research, encompassing a series of 25 beach-profile surveys conducted with an average 2-week interval. One particularity of this dataset is the integration of high-resolution, 30-minute imagery and video that (1) captures the degree of inundation across the berm that is not captured in typical coastal datasets and (2) provides an unprecedented level of detail in capturing the dynamic evolution of the coastal landscape. Creating this dataset is an academic endeavor and a response to the practical needs of beach managers and conservationists. By establishing a regular survey schedule and incorporating continuous monitoring through imagery and video, the goal is to provide a foundation for understanding the intricacies of beach morphology changes in real-world conditions. This meticulous approach enables researchers to capture the gradual change in beach-profile morphology, the influence and correlation to periodic inundation events, and the mechanisms responsible for them.

In the subsequent sections of this paper, the methodology employed in data collection is explored, highlighting the systematic approach and the technology used. The paper also presents results and discussions, shedding light on the unique insights gained from the analysis of this comprehensive dataset. Ultimately, this work contributes to the broader discourse on coastal management, offering an improved understanding of beach morphology changes that can inform sustainable practices and decision-making.

UNDERSTANDING LOCAL COASTAL DYNAMICS: COASTAL INUNDATION AND TYPICAL EROSION

In this section, the fundamental forces driving coastal dynamics are explored, examining two interconnected phenomena: coastal inundation and typical coastal erosion. The goal of discussing these topics is to provide an understanding of the transformative mechanisms that shape the interface between land and sea in coastal environments.

Coastal Inundation

Coastal inundation is a natural process characterized by submerging coastal areas, presenting a complex interplay of environmental factors. This phenomenon occurs because of the combined dynamic forces of wind, waves, tides, and currents, leading to the encroachment of water across the typically subaerial beach, including the foreshore, berm, and backshore (Hague and Taylor, 2021; Krestenitis *et al.*, 2011; Wang *et al.*, 2020). This study specifically focuses on coastal processes influencing the inundation of the berm along a wide recreational beach.

Coastal inundation has far-reaching consequences, affecting natural ecosystems and coastal communities (Mcinnes *et al.*, 2003). The encroachment of water onto land can result in the temporary submersion of low-lying areas, affecting habitats and disrupting ecosystems. Furthermore, human infrastructure (*e.g.*, homes, roads, businesses) may be at risk during inundation events, leading to potential economic and societal impacts (Jeon, Eem, and Park, 2018; Wang *et al.*, 2020). Finally, coastal inundation may result in limitations on emergency and public access to essential resources. Although coastal inundation is a distinct process from erosion, its occurrence can influence erosion dynamics (Pollard, Spencer, and Brooks, 2019). In some cases, inundation may contribute to erosion by altering sediment transport patterns and affecting coastal features (Fabiyi and Yesuf, 2016). However, not all instances of inundation lead to erosion, and the relationship between the two processes depends on various factors, such as the duration, intensity, and frequency of the inundation event (Pollard, Spencer, and Brooks, 2019).

Coastal Erosion

Coastal erosion, driven by natural forcing mechanisms such as wind, waves, tides, currents and sea-level rise, influences sediment transport and the morphology of coastal landforms (Gillie, 1997; Prasad and Kumar, 2014; van Rijn, 2011). Erosion is a natural process characterized by gradually eroding and reshaping shorelines, cliffs, and beaches due to the relentless forces of these elements (Saadon *et al.*, 2020) and anthropogenic influences in some areas. The dynamic interactions of wind, waves, tides, and currents may manifest in the gradual landward recession, also referred to as "retreat" or complete elimination of coastal features (Gillie, 1997; Prasad and Kumar, 2014; Prasetya, 2007; van Rijn, 2011). Wave action, influenced by wind patterns, at times combined with surge events, erodes landforms such as the berm or dunes by persistently transporting and depositing sediment along and across the shore (Prasad and Kumar, 2014). Additionally, sea-level fluctuations, influenced by tides and climatic conditions, contribute to the erosive impact by altering wave

energy and frequently shifting the focus of coastal forcing further onshore (Prasetya, 2007; van Rijn, 2011). Geological factors, including the type of coastal sediment and bedrock composition, further influence erosion rates, portraying coastal erosion as a dynamic and intricate phenomenon (Saadon *et al.*, 2020).

It is necessary to recognize that coastal erosion can be transitory and episodic, particularly in areas characterized by unconsolidated materials such as sand, pebbles, and shells, constituting a soft coast (Prasetya, 2007). These regions, typically dissipative beaches, are characterized by short-term fluctuating or cyclic erosion, requiring long-term assessments to quantify the degree of erosion and persistence of the problem (Prasetya, 2007). Dissipative beaches with flat slopes and wide barred nearshore shelves are found along Gulf-facing beaches along the Texas coast. Despite experiencing erosional events, accretion and dune rebuilding along such soft coastal environments can take an extended period, potentially leading to insufficient time for natural beach recovery before the next erosive event occurs (Prasetya, 2007; Williams and Turner, 2022), with a possible the frequency increase. This increase potentially leads to the need for cyclic beach nourishment, which is common on many Texas Gulf coast beaches.

Study Area

Measurements were conducted along a small 55×85-m segment of the Gulf-facing beach that is adjacent to Horace Caldwell Pier, Port Aransas, Texas. The study area—found along a small segment of the I.B. Magee Beach Park and managed by Nueces County Coastal Parks—is located south of the Aransas Ship Channel south jetty on Mustang Island, a 29-km long barrier island along the central Texas coastline. The study area is closed to vehicles, whereas the surrounding beaches are mostly open to traffic, both in accordance with the Open Beaches Act and Texas law (Texas Natural Resources Code, 2024). Therefore, the study area's beach morphology is more natural than most other beaches along Mustang Island, with the exception of a segment of Mustang Island State Park, because of infrequent mechanical redistribution of sand and lack of vehicular traffic. A small trench constructed on the southern end of the study area is maintained by park staff to help promote pier access by reducing pooling after rain and periods of inundation.

The focused area of study begins seaward of the parking area and extends across the central berm, ending at the water's edge at the time of data collection, which is variable (Figure 1). The beach segment stretching from the south jetty to Lantana Drive has been relatively stable since the 1950s (Morton and Pieper, 1977; Gibeaut *et al.*, 2001; Williams and Turner, 2022); it historically was blocked by the construction of Aransas Pass and is associated with approximately 1.5 km long jetties completed during 1919. The median grain size ranges from 0.16 mm at the dunes and midshore to 0.18 mm at the surf, with a slope of 0.02 m (Knezek, 1997). Sediment transport along Magee Beach is primarily influenced by longshore sediment transport directed toward the NE during strong SE winds that dominate most of the year. Exceptions occur during winter storms and tropical events when cross-shore sediment transport dominates due to onshore surges and storm waves. The berm near the south jetty is significantly wider than the adjacent beach to the south, generally decreasing in width with distance from the jetties at Aransas Pass.

The berm near the south jetty has been relatively stable since its construction, except for periods of hurricane impact. The beach exhibits periodic, event-driven erosion during hurricanes and tropical storms but is generally stable and has demonstrated recovery following storms of significance. This includes the impact of 2017 Hurricane Harvey, which created significant beach erosion close to the jetty and a breach of the jetty, yet recovery took place without beach renourishment or other anthropogenic action (Williams and Turner, 2022).

Unique Characteristics of the Study Area

The unique characteristics of the designated research study area and the implications for generalizing results to other coastal contexts are outlined here. Sediment transport in the study area is influenced by wave shadowing, refraction, and human activities associated with the proximity of Horace Caldwell Pier and the long south jetty. The south jetty shelters the adjacent beach from longshore currents directed from the north, thereby influencing alongshore sediment transport as well as impoundment. The isolated location minimizes mechanical sand management of the berm and limits vehicular access that can disrupt natural sediment transport, leading to a more natural dataset. Additionally, the study area is wider and has a higher elevation than other beaches on Mustang Island, leading to less frequent periods of inundation that reach the dune line. These factors highlight the need for careful interpretation of results, considering the influence of coastal structures and differences in beach management in the study area as compared with the adjacent beaches. In addition, this paper also provides the basis for a recommended more detailed analysis of anthropogenic influences on beach stability in future studies.

Anthropogenic Impact

The ways in which anthropogenic structures (*e.g.*, piers and jetties) and restricted vehicular access influence the study area's beach morphology are examined here. Understanding these impacts is necessary for accurately interpreting and generalizing the results of this study.

The proximity of Horace Caldwell Pier to the study area introduces several distinct influences on beach morphology. First, the pier contributes to wave shadowing and refraction dynamics because it can cast a shadow that alters the distribution of wave energy along the beach (Miller and Dean, 2004; Splinter *et al.*, 2014). Additionally, waves refracting around the pier may generate areas of heightened energy or turbulence, potentially leading to localized erosion or accretion (Ludka *et al.*, 2015; Pianca, Holman, and Siegle, 2015; Plant *et al.*, 1999). Second, the structural impact of piers on sediment transport is notable, acting as barriers that disrupt the natural alongshore movement of sediment (Splinter *et al.*, 2014). This disruption can result in the accumulation of sand on one side of the pier and erosion on the other, emphasizing the need for an understanding of localized sediment dynamics (Splinter *et al.*, 2014).

Similarly, the influence of the nearby jetty on beach morphology is multifaceted. First, the jetty provides a sheltering

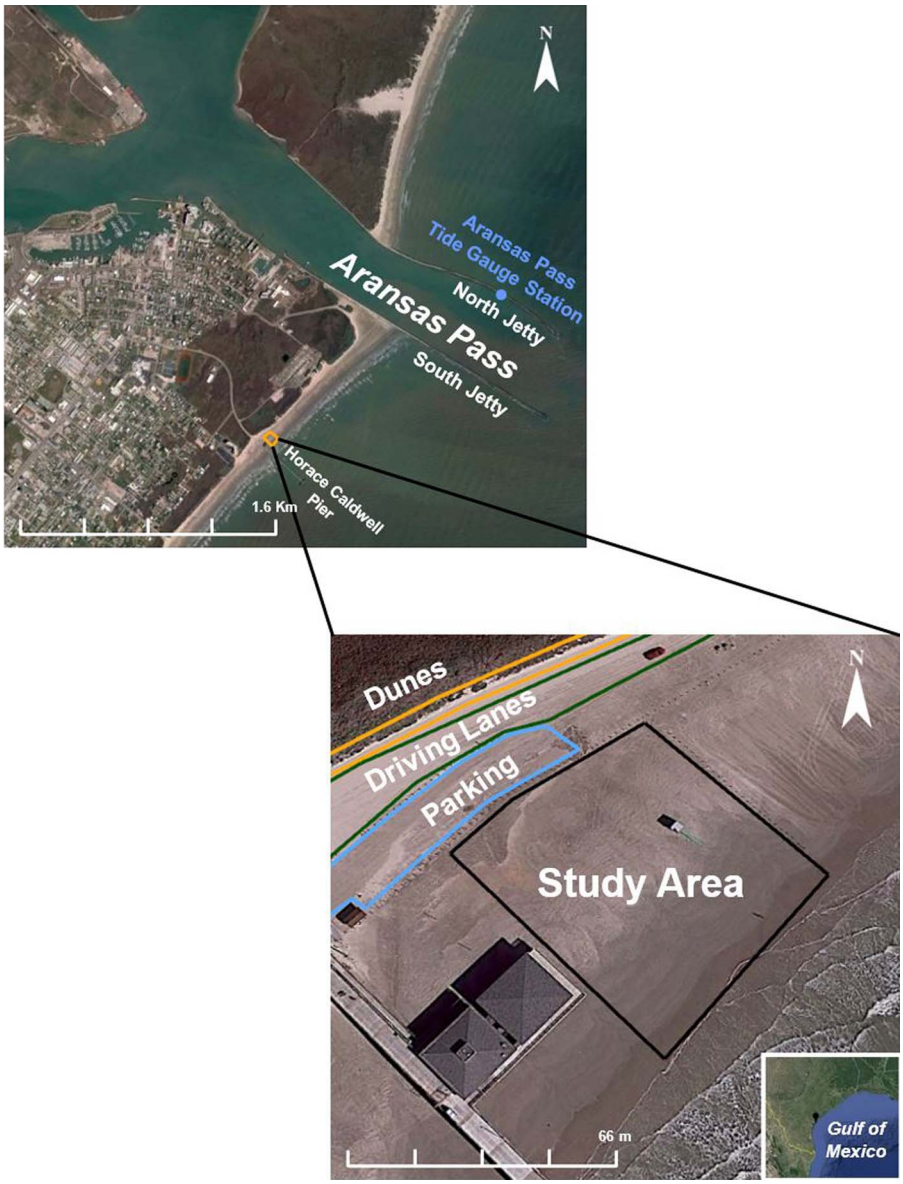

Figure 1. The figure illustrates the study area, situated adjacent to and north of Horace Caldwell Pier, Port Aransas, Texas. The image highlights the surveyed region (study area), the parking zone, the beach driving lanes, and the nearby dunes. A view of the bollards, which serve to delimit traffic boundaries in the area, is also provided.

effect on the adjacent beach, protecting it from the full impact of longshore sediment transport directed from the NE and influencing natural sedimentary processes (Garel, Sousa, and Ferreira, 2015). It has been observed that the dominant direction of sediment transport is from south to north because of dominant winds directed from the S to SE (Fox and Davis, 1978; Hunter, Richmond, and Alpha, 1983; Knight and Burningham, 2003).

Second, the impoundment of sediment by the jetty design contributes to variations in sediment availability and distribution along the beach (Garel, Sousa, and Ferreira, 2015). Understanding the historical context of jetty construction is critical for interpreting the long-term stability of the beach in relation to sediment dynamics. Garel, Sousa, and Ferreira (2015) showed that erosion of historical deltas can influence updrift shoreline progradation and sand bypassing after jetty construction. Furthermore, Suanez *et al.* (2015) highlighted that the construction of jetties can lead to hydrodynamic modifications and interrupted sand drift, resulting in increased sediment loss for beach and dune systems. Additionally, Gordon and Nielsen (2020) emphasized that jetties at estuary entrances have the potential to induce fundamental coastal and estuary process alterations, which may take centuries to resolve.

Finally, Texas beaches typically allow vehicular traffic, complicating the interpretation of natural beach morphology changes due to mechanical sand redistribution by the vehicles themselves and also during the efforts to manage beach driving lanes and parking areas. This study focused on a protected area that prohibits public driving, thereby minimizing mechanical sand redistribution and enhancing data reliability. Although occasional use by lifeguards and beach managers occurs, the area experiences significantly less interference from continuous vehicular traffic and the beach management associated with it. This characteristic distinguishes the study area from most Texas Gulf–facing beaches, offering a clearer understanding of beach changes without ongoing vehicle-driven activities and maintenance operations.

The study area is limited to the unaltered berm, excluding profiles landward of the parking area where anthropogenic influences begin. This focus preserves data integrity, avoiding variability from areas accessible to cars. The influence of runup rarely extends to the road and dunes, except during the impact of Hurricane Ian reaching the Texas coast on 29 September 2022. This strategic focus on a minimally influenced study area enhances the reliability of findings, removes unknown influences, and provides valuable insights into beach dynamics in a relatively undisturbed coastal environment.

Microtidal Range

The effect of tidal dynamics on the study area introduces another feature that distinguishes the study area from some other coastal research settings. The Texas coast has a limited tidal range with, for example, a mean range of tides (MN) of 0.36 m within the Galveston ship channel entrance jetties, 0.40 m for Corpus Christi, and 0.38 m within the Brazos Santiago Pass (NOAA, 2023a). The range of the seasonal cycles is similar to the tidal range: 0.27 m for the Galveston Ship channel 0.27 m for Aransas Pass (NOAA, 2023b, c). The range of the daily water level is often driven by meteorological forces, particularly wind more so than tidal influence. Despite the limited tidal range, tides significantly influence the erosion of the foreshore and berm when combined with wind, surge, and wave forcing, particularly because of the flat slope of Texas beaches.

The influence of low tide is particularly noteworthy, exposing a significant portion of the foreshore and berm to direct coastal processes (Coco *et al.*, 2004). This exposes formerly submerged areas to strong onshore waves, altering the typically protected foreshore. Low tide's temporal variability captures distinct beach morphology changes (Bernabeu Tello, Medina Santamaría, Vidal Pascual, 2002). Furthermore, the low tide conditions in the study area influence sediment transport patterns. With a wider foreshore exposed during low tide, sediment movement and redistribution may exhibit greater variation compared to high tide conditions (Carrasco *et al.*, 2011). The ebb and flow of tidal currents play a role in shaping the nearshore bathymetry, influencing the deposition and erosion of sediment (Pacheco *et al.*, 2015). This temporal variability adds a layer of complexity to the dataset, offering insights into the way in which tidal stages contribute to the overall dynamics driving changes in beach morphology.

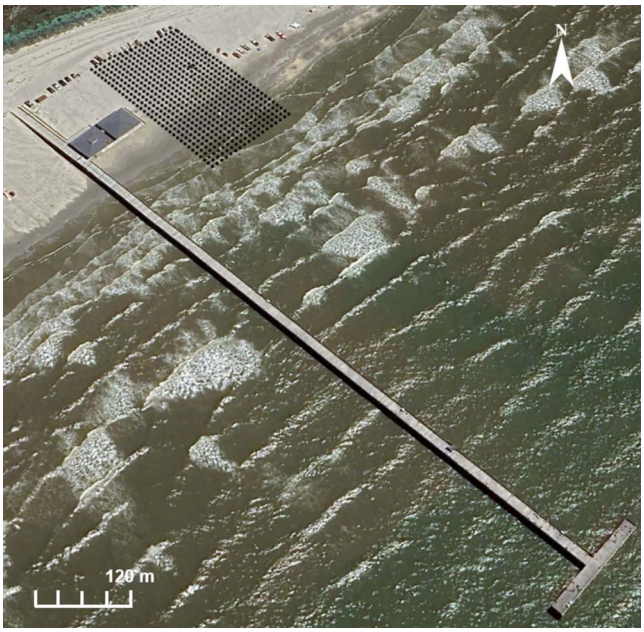

Figure 2. Location of the study area next to Horace Caldwell Pier (top) with data points (grid) collected during one of the surveys, which is representative of all surveys conducted at Horace Caldwell Pier.

METHODS

The methodology employed in this research included conducting 25 beach-profile surveys with an average 2-week interval between each survey. In addition, a set of cameras was strategically installed to monitor the study area continuously. The data from the cameras provided valuable information because it allowed the recording and observation of inundation events, which can contribute to beach erosion and are rarely captured by other datasets. The elevation measurements acquired during these surveys were applied to develop beach-profile plots. These plots showed the pre- and postevent state of the berm as well as change over the extended study period, serving as a fundamental component for the analysis and interpretation of changes in beach morphology over the study period.

Data Collection

The modified beach-profile surveys were conducted using a Trimble R10 Global Navigation Satellite System receiver equipped with virtual reference stations to measure topographic spot elevations along the beach through real-time kinematic positioning. The beach-profile survey extent is modified because of the focus covering only the most dynamic section of the berm and foreshore.

A systematic approach was adopted, employing a 3.05×3.05 m grid (10×10 ft; Figure 2). The x and y coordinates were referenced to NAD 1983 State Plane Texas South, whereas NAVD88 (GEOID12B) was used for elevation measurements. All survey grids shared a common starting point; however, the termination of each survey, particularly in proximity to the water, was contingent upon the fluctuating position of the water line during the survey, resulting in surveys of varying lengths.

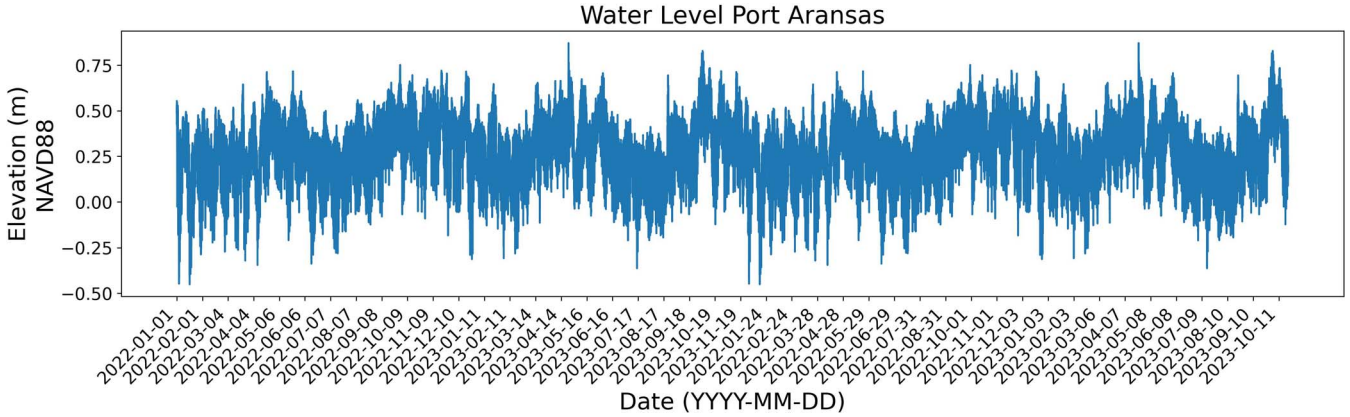

Figure 3. Representation of hourly Port Aransas water-level signal.

The survey area includes the berm and foreshore but does not include the backshore or backshore limiting features such as dunes. Therefore, the profile section is truncated and not representative of the entire region of sediment transport but instead captures the most dynamic region during inundation.

The survey campaign commenced on 7 July 2022 and concluded with the last survey on 13 September 2023. Throughout this timeframe, surveys were conducted regularly, with an average frequency of 2 weeks. The shortest interval between surveys was 1 week, while the longest extended to approximately 1 month. This survey schedule allowed for a comprehensive and temporally diverse dataset, enabling a thorough examination of beach elevation and morphology over the specified period.

Beach Profiles

The application of beach-profile survey data is a fundamental methodology for analyzing temporal changes in beach morphology. These profiles facilitate quantitative and qualitative assessment, capturing the intricate dynamics inherent in coastal environments. By generating beach profiles from surveys conducted to document distinct conditions, this approach enables direct temporal comparison, unveiling trends and understanding the impact of natural and anthropogenic factors on beach dynamics. This quantitative approach is a valuable tool for identifying trends in erosion and accretion, offering insights into how the beach responds to environmental changes and providing a foundation for informed decision-making in coastal planning and management.

An average beach profile was computed for each survey by averaging the elevation measurements of all the survey points for each alongshore row. The variability of the beach elevations along each row was estimated using two standard errors. The two standard errors were found to be very small, with a mean value of 1.7 cm. This measure of limited variability confirms that the alongshore beach morphology is relatively homogeneous when moving from the water line toward the dunes and that anthropogenic impacts or other forcings do not substantially influence the measurements and natural beach dynamics. Note that although the starting point of the survey lines was consistent, the width of each beach profile varied because of its termination point at the water line at the time of the survey. The surveys were conducted under various tidal conditions, with some surveys occurring during low tide and others during high tide. This disparity in tidal levels, along with the other factors driving water-level variability, influenced the length of the beach profiles, with surveys during periods of high water level resulting in shorter profiles. The temporal variability, along with the differences in the offshore limit of data collection, presents a limitation in the interpretation of the data, which is acknowledged, although the random nature of the surveys allowed for unexpected events to be documented. Ideally, surveys would have been conducted during peak low tides and extended further into the nearshore, but, given the relatively high frequency of the surveys, limitations in seaward extent occurred because of scheduling constraints.

Meteocean Data

This section describes the influence of metocean conditions on the occurrence of beach inundation and under specific conditions in combination with erosion. To gain deeper insights into this influence within the dataset, a thorough analysis of metocean conditions was conducted, encompassing wind speed and direction, water level, and wave data. Hourly water-level data from Aransas Pass was chosen for analysis because of proximity (about 1600 m) to the study area (National Oceanic and Atmospheric Administration, 2023g; Figure 3). Wind measurements were from the National Data Buoy Center (NDBC) C-Man station located on the seaward side of Horace Caldwell Pier, the PTAT2 station (NOAA, 2023f). Options regarding wave data were limited because no stations or buoys were close to the study area. At the time of this writing, no buoys measuring nearshore wave conditions are found anywhere along the Texas coast, making such studies and the design of coastal structures more difficult. The available choices were measured waves from buoys NDBC 42019 (National Oceanic and Atmospheric Administration, 2023d) and NDBC 42020 (National Oceanic and Atmospheric Administration, 2023e) and buoy stations and reanalysis data from station ST73039 from the WaveWIS portal (USACE, 2023b). Of these, the WaveWIS portal provides data closest to

Figure 4. Location of the wave buoy stations in the Gulf of Mexico with respect to the study area.

the coast. Still, the data are limited to 2022 and previous years, limiting applicability to interpreting results for most of the surveys conducted in 2023. In contrast, although more offshore than ideal, NDBC 42019 and 42020 buoy data offer available data up to present date (Figure 4). Consequently, these two sources constitute the only wave data available for the analysis.

The NDBC 42019 station is situated north of the study area, whereas NDBC 42020 is located to the south, a bit closer to the coast. Depending on wave directions, one buoy's data may be more representative of onshore conditions close to the study area than the other. Thus, both buoys are considered valuable; determining which buoy provides more accurate and valuable information depends on the wave direction. Consequently, a decision was made to create a wave signal incorporating the maximum values from both buoys. This approach was chosen because the largest wave conditions are most influenced by inundation and erosion events. Typically, these events are triggered by individual occurrences with higher values than the average rather than by the average values. Figure 5 illustrates the hourly maximum significant wave height, maximum average wave period, and maximum dominant wave period, respectively, obtained from combining the maximum values from the two buoy stations.

Figures 3, 5, and 6 illustrate the fluctuations in water-level measurements, waves, and winds during the study period. The influence of tides, winds, seasonality of metocean parameters, and more extreme events can be identified. The visual representations emphasize the need for a deeper exploration of the impact caused by the high peaks of waves and water level in the study area. A detailed discussion on this matter is provided in the "Results" and "Discussion" sections.

RESULTS

The results of the combined analysis of changes in consecutive beach profiles and metocean variables describes the morphological dynamics of the study area. The results also compare the beach profiles of the first and last surveys of the dataset to provide analysis of annual change. This analysis provided the basis for a detailed examination of the seven full and partial beach inundation cases documented during the study period ("Discussion" section).

Morphological Dynamics of the Study Area

This section describes changes in beach-profile morphology over 19 paired sets of consecutive surveys spanning a period of 12 months. The spatial variability in the measurement of beach morphology is estimated using two standard errors of the mean alongshore survey measurements. The variability is represented by the lighter band color (ribbon) in Figures 7-10. For most cases, minor differences occur in the morphology of consecutive beach profiles (Figure 7a,b); however, events with high dominant wave periods (*e.g.*, Figure 7c–e) cause erosion on the foreshore with sand redistribution across the landward section of the berm (discussed further in the "Inundation Cases" section).

Inundation Cases

In addition to frequent beach surveys, the study was enhanced by deploying cameras to continuously monitor the study area. The images and videos allowed real-time

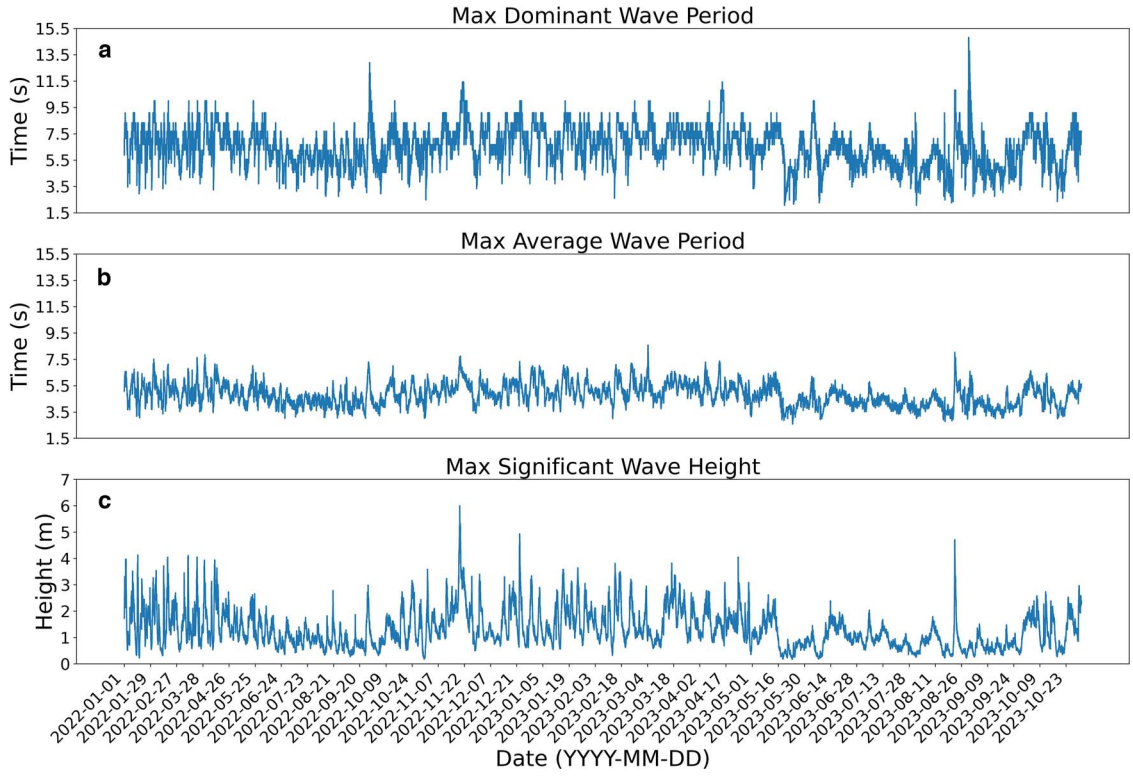

Figure 5. Illustration of (a) maximum significant wave height, (b) maximum average wave period, and (c) maximum dominant wave period. Values obtained after combining NDBC 42019 and NDBC 42020 data.

observation of the dynamic interplay between water, waves, and the beach, determining how far landward the water advanced across the berm. Seven full inundation or partial events were identified, characterized either as water covering the beach up to the bollards next to the driving lane and back dunes or water covering up to the middle of the berm without reaching the bollards, respectively. These events are listed and further described in Table 1.

Figures 11 and 12 present the respective metocean conditions during the inundation events identified in Table 1. The relationship between the inundation events and the metocean forcings is described in the "Discussion" section.

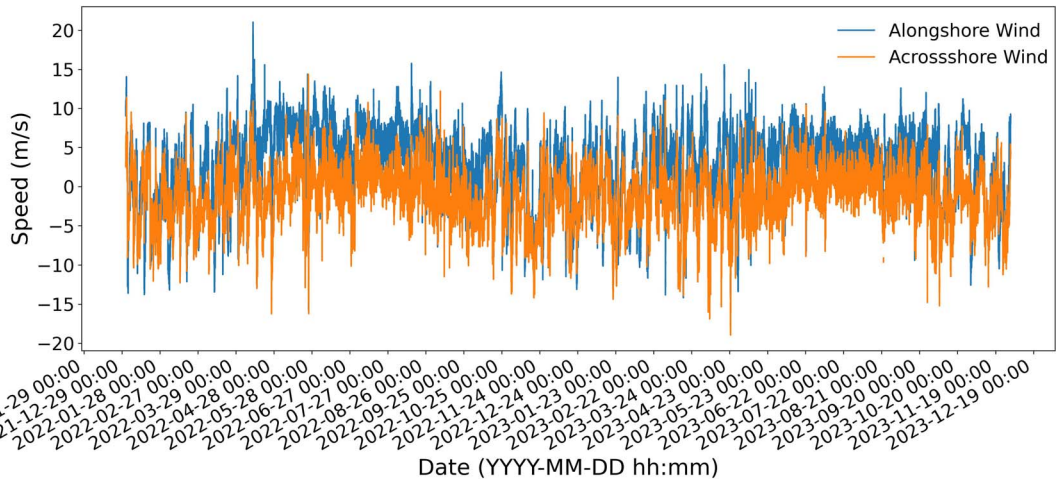

Figure 6. Alongshore and across-shore wind speeds measured at the NDBC PTAT2 station located on the seaward end of Horace Caldwell Pier.

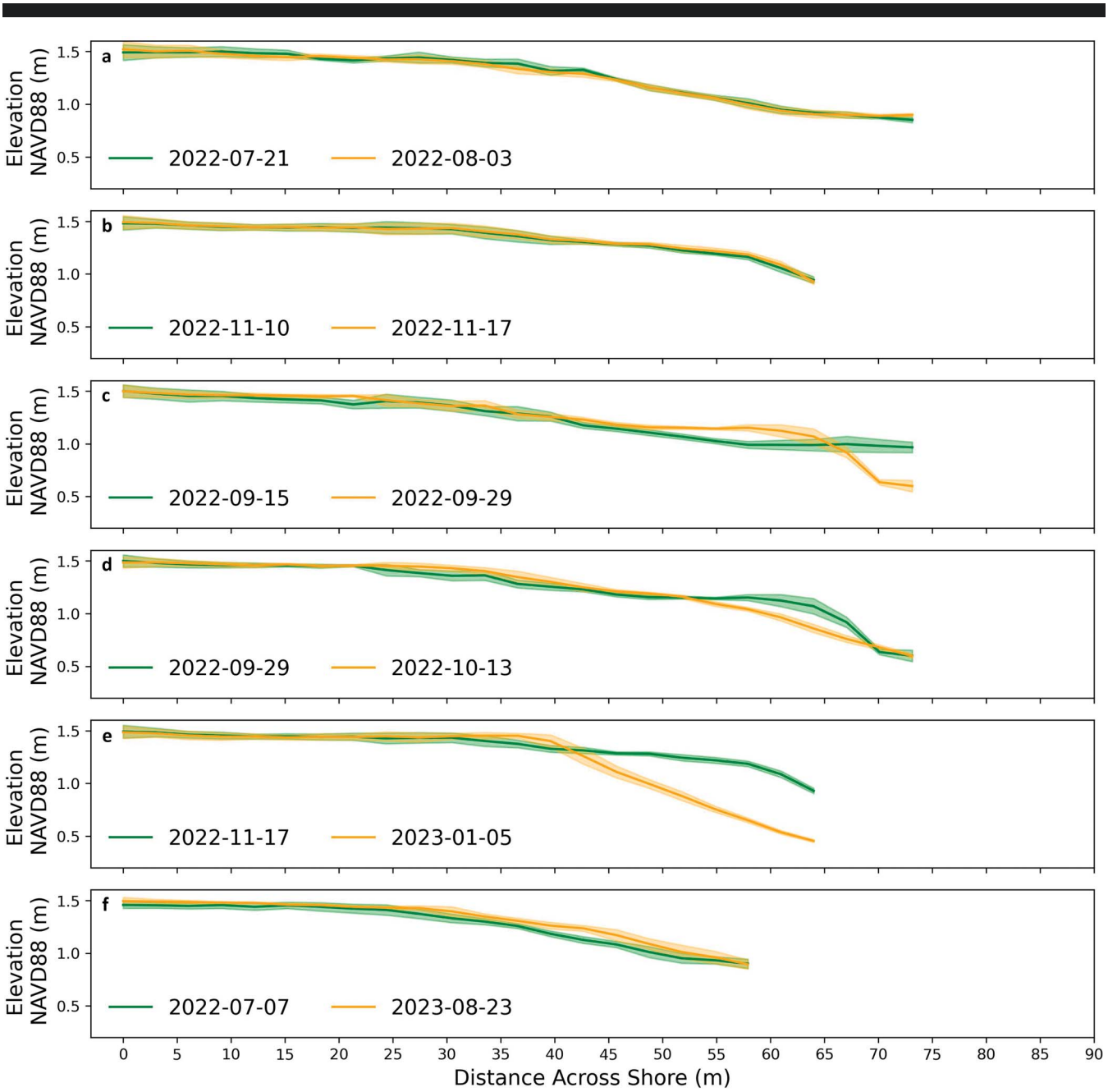

Figure 7. Comparison of beach profiles from two consecutive surveys: (a) 21 July 2022 and 3 August 2022; (b) 10 and 17 November 2022. They are representative of the most common beach morphological changes between two consecutive surveys. (c) Impact of Hurricane Ian on 29 September 2022 during its initial hours; (d) impact of Hurricane Ian on beach morphology; (e) erosion on the foreshore due to high dominant wave period; (f) comparison of the first and last beach profiles, indicating stability.

Figures 8, 12, and 10—detailing Cases 1, 2, and 3, respectively—illustrate the shoreline camera imagery during inundation events along with the changes in beach topography associated with these events. Figures 13, 14, and 15—detailing Cases 1, 2, and 3, respectively—display time series of wind speeds and wind directions measured during the respective events at the study site.

Figure 16 displays the total water-level time series results for the study period and compares it with the average water levels measured at the nearby tide gauge and the associated harmonic predictions. The time series are also compared with the highest astronomical tide (HAT), the mean high water (MHW), and the mean higher high water (MHHW) tidal datums for the study area tide gauge station.

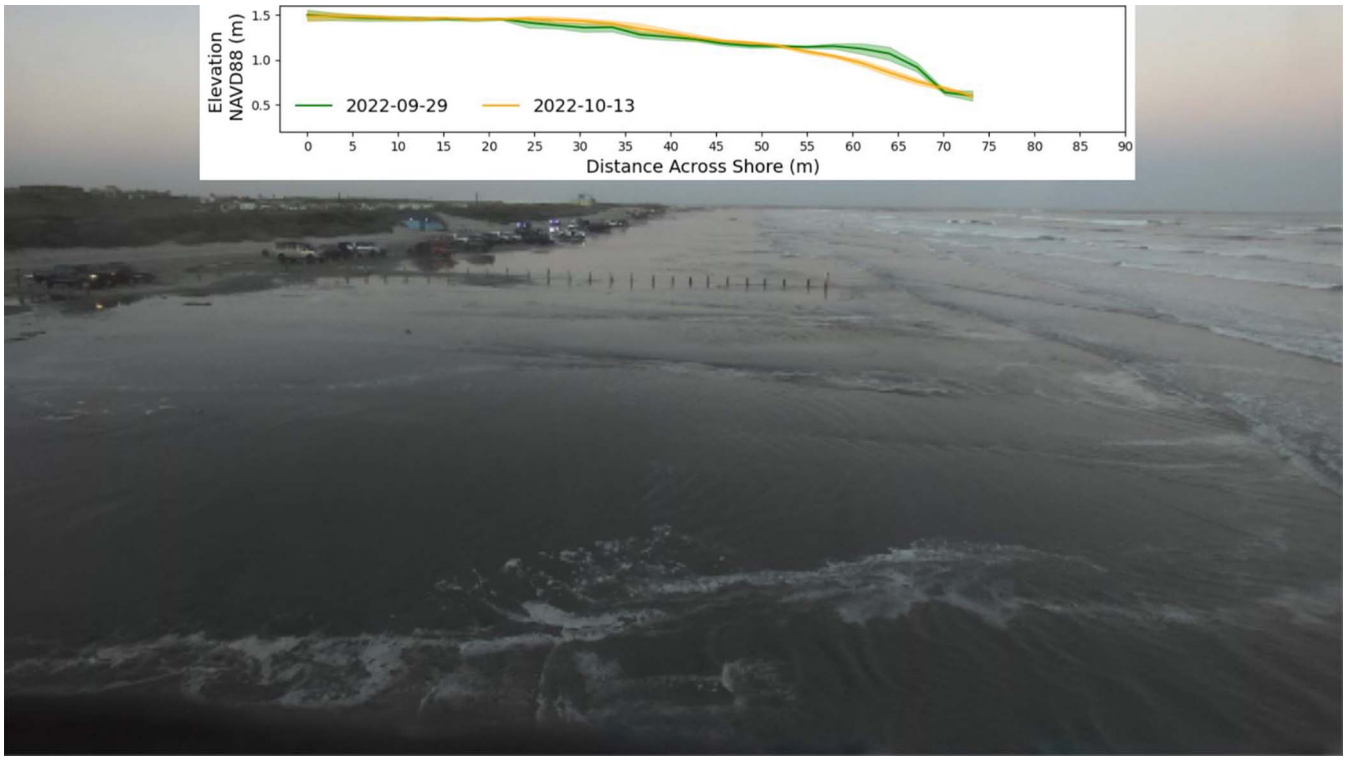

Figure 8. Degree of inundation during Hurricane Ian on 29 September 2022 (1720 [central daylight time]). The beach profile inserted at the top of the figure illustrates erosion across the foreshore that occurred during by Hurricane Ian.

DISCUSSION

This section provides a detailed analysis of the seven full and partial beach inundation cases documented during the study period. These events were associated with increases in the maximum dominant wave period, maximum significant wave height, and water level. A maximum dominant wave period threshold of approximately 10 seconds was found to be associated with a high risk of full or partial beach erosion across the berm in the study location. The discussion concludes with the comparison of the wet/dry shoreline elevation with tidal datums. Through this discussion, a pattern emerged that revealed that the location of the wet/dry shoreline consistently exceeded the MHW and MHHW elevation. Furthermore, the wet/dry shoreline remained predominantly above the HAT elevation. Collectively, these findings contribute to a deeper understanding of the dynamic interactions within the study area and future coastal modeling applications.

Discussion of Inundation Cases

To enhance the understanding of the inundation events, the inter-relationship between metocean variables (*e.g.*, maximum significant wave height, maximum average wave period, maximum dominant wave period, average water level) were analyzed during instances of inundation (Figures 11 and 12); each inundation case, detailed in the "Results" section (Table 1), is visually in both figures. The varying widths of these columns correspond to the respective durations of the inundation events, with wider bands indicating longer-lasting events. A detailed examination of each inundation case follows.

Inundation Case 1

Inundation Case 1 describes an event that occurred between 29 and 30 September 2022, which correlated with the landfall of Hurricane Ian on the other side of the Gulf of Mexico on Cayo Costa Island, SW Florida. Figures 11 and 12 illustrate that the maximum significant wave height, maximum average wave period, maximum dominant wave period, and average water level are all significantly above their averages, suggesting their significant role in beach inundation. The study's maximum average wave period is recorded during the landfall of Hurricane Ian.

Figure 8 shows the study area fully flooded during this event, with water reaching the bollards. Figure 13 describes nearshore winds at 5–6 m/s during the 4 to 5 hours preceding the image shared in Figure 8. Stronger nearshore winds were also recorded (reaching up to 8 m/s from the same direction), but about 24 hours earlier, and not thought to have contributed directly to this inundation event. Further analysis of the lack of direct nearshore wind influence on the inundation of this beach is discussed at the end of this section.

Figure 7c, d illustrates the impact of Hurricane Ian on the beach morphology. On 29 September, the survey was conducted a few hours after the impact of Hurricane Ian started. This beach profile shows foreshore erosion and sand redistribution landward, as compared with the prior profile correlated with a long maximum dominant wave period exceeding 10 seconds

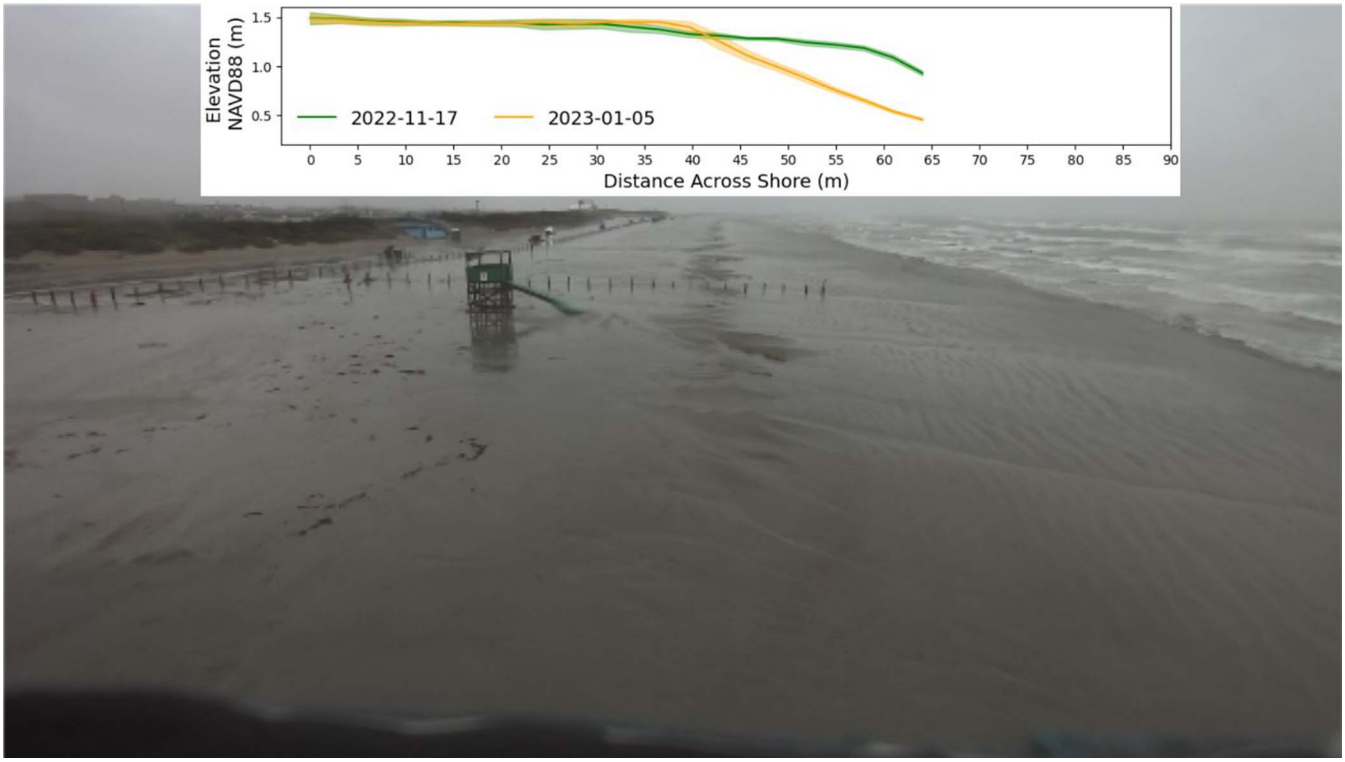

Figure 9. Inundation event on 19 November 2022 (1400 [central daylight time]). The beach profile at the top of the figure illustrates the foreshore erosion consistent with the long, dominant wave period.

(Figure 7c). Figure 7d compares the beach morphologies a few hours after the initial impact of Hurricane Ian and 2 weeks later. This comparison shows further foreshore erosion and landward sand redistribution. Despite Hurricane Ian causing full beach inundation, only the foreshore experienced erosion.

Inundation Case 2

Inundation Case 2 occurred on 19 November 2022. The fully flooded beach is illustrated in Figure 9. To understand this event, a thorough data examination was performed, focusing on the maximum significant wave height (Figure 7a), maximum average wave period (Figure 7b), and maximum dominant wave period (Figure 7c), derived from the combined datasets of NDBC 42019 and NDBC 42020. Additionally, the water level at Aransas Pass was studied (Figure 12). Similar to inundation Case 1, this inundation event is characterized by elevated values in maximum significant wave height, maximum average wave period, and water level—inundation-driven factors that pushed the water inland. The impact of these elevated values is further illustrated in Figure 7e, illustrating significant foreshore erosion with sand redistribution landward (Figure 9). Similar to the previous inundation event, the dominant wave period was more than 10 seconds.

Inundation Case 3

The third recorded inundation event, documented on video on 18 January 2023 (Figure 10), unfolded under similar conditions to inundation Case 2. Mirroring the patterns observed in this earlier event, an increase in maximum significant wave height (reaching 10 seconds), maximum average wave period, and average water level occurred, resulting in the inundation of the full beach. The beach profiles in Figure 10 illustrate a small degree of foreshore erosion with sand redistribution across the berm in a landward direction. Figure 15 describes relatively light nearshore winds in the 1–8 m/s range, mostly from the south with a short shift to the north for a few hours on 17 January, about 24 hours before the image of the beach in Figure 10.

Inundation Cases 4 through 7

Specific figures documenting inundation Cases 4 through 7 are not included in this text but are subsequently described and compared with the prior cases. These events occurred in 2022 on 14 February, 16 and 17 March, 13 April, and 24 and 25 April (Table 1). For all cases, increases in maximum wave height, maximum average wave period, and water levels were observed, leading to full or partial beach inundations. Cases 4 and 5 were the only inundation events without beach erosion. Figure 11 show that these two cases, along with Case 7, show a maximum dominant wave period under 10 seconds.

Although a maximum dominant wave period of only 8.3 seconds was recorded for Case 7, the highest water levels of the study were recorded during this event (Figure 12), likely compensating for the lower maximum dominant wave period and explaining the onset of partial beach erosion. For Case 6,

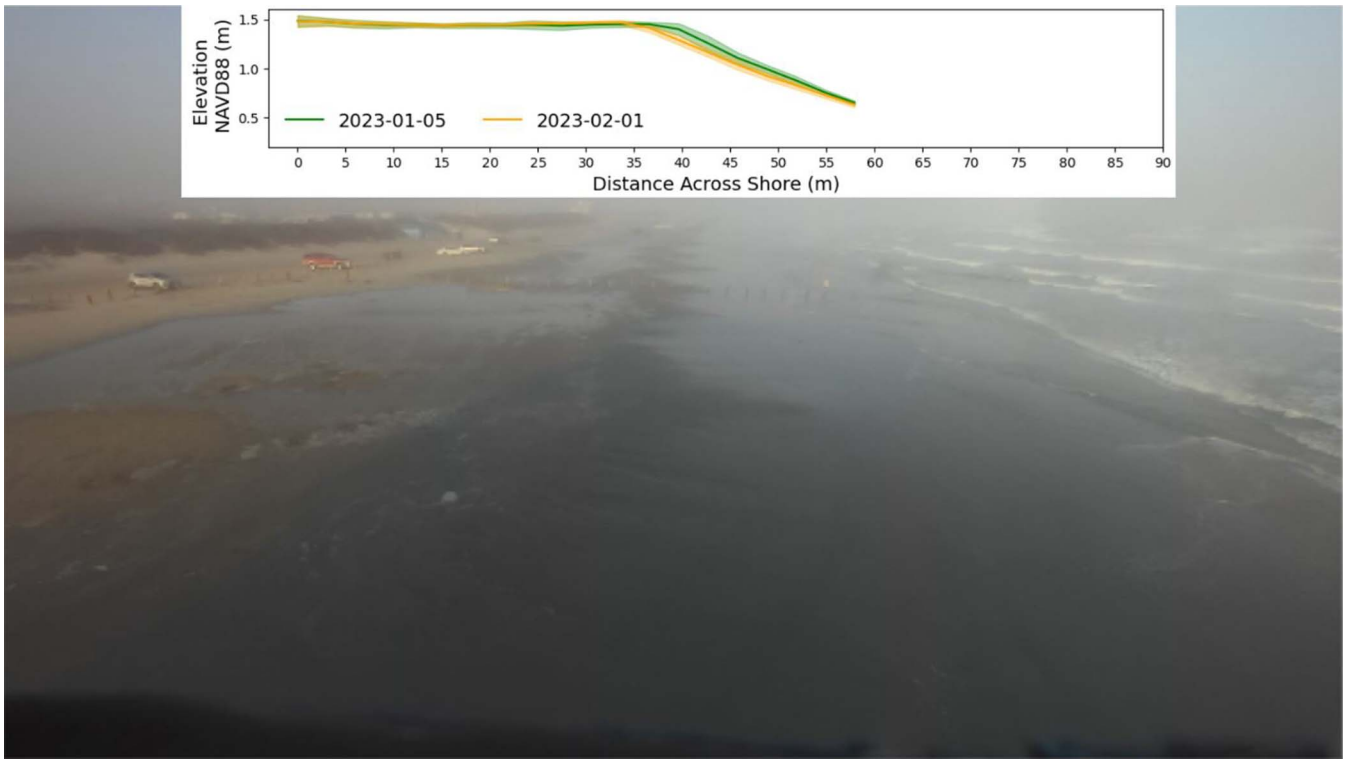

Figure 10. Facing north from Horace Caldwell Pier: inundation event on 18 January 2023 (1400 [central daylight time]). The beach profile at the top of the figure illustrates the small foreshore erosion consistent with the long-dominant wave period.

the maximum dominant wave period was more than 10 seconds with foreshore erosion, similar to Cases 1 and 2. This suggests that a maximum dominant wave period threshold of 10 seconds leads to erosion by itself but that very high water levels and potentially other metocean variables, such as very high maximum significant wave height, can be compounded to create erosion at a maximum dominant wave period slightly under the 10 seconds threshold. This statement holds for the beach profiles compared during the entire study period.

Maximum wind speeds during Cases 4 through 7 reached, respectively, about 12, 15, 4, and 10 m/s with wind directions, respectively, from the S, N, SE, and N at the time of the maximum wind speed observed. Maximum wind speeds during Cases 1 through 3 were 6, 16, and 8 m/s from the north and south, respectively. Although this part of the Texas coast experiences some of the strongest nearshore wind speeds in the continental coastal United States and winds play a significant role in the dynamic of nearshore currents and waves as well as water levels, nearshore winds were not identified as a major driving factor regarding inundation and erosion of the beach during this study. The findings from these additional cases reinforce the consistency of these patterns, providing further support for understanding

Table 1. *Beach inundation cases identified through a review of the beach imagery and correlated drivers of coastal inundations.*

Case Number	Date of Event	Event	Supplementary Information
1	29 and 30 September 2022	Full beach inundation with erosion across the foreshore (Hurricane Ian)	https://github.com/conrad-blucher-institute/High-Resolution-Beach-Morphodynamics/tree/main/Inundation%20Event%20%231
2	19 November 2022	Full beach inundation with erosion across the foreshore	https://github.com/conrad-blucher-institute/High-Resolution-Beach-Morphodynamics/tree/main/Inundation%20Event%20%232
3	16 and 18 January 2023	Partial beach inundation with small erosion across the foreshore	https://github.com/conrad-blucher-institute/High-Resolution-Beach-Morphodynamics/tree/main/Inundation%20Event%20%233
4	14 February 2023	Partial beach inundation without erosion	https://github.com/conrad-blucher-institute/High-Resolution-Beach-Morphodynamics/tree/main/Inundation%20Event%20%234
5	16 and 17 March 2023	Full beach inundation without erosion	https://github.com/conrad-blucher-institute/High-Resolution-Beach-Morphodynamics/tree/main/Inundation%20Event%20%235
6	13 April 2023	Partial beach inundation with small erosion across the foreshore	https://github.com/conrad-blucher-institute/High-Resolution-Beach-Morphodynamics/tree/main/Inundation%20Event%20%236
7	24 and 25 April 2023	Partial beach inundation with small erosion across the foreshore	https://github.com/conrad-blucher-institute/High-Resolution-Beach-Morphodynamics/tree/main/Inundation%20Event%20%237

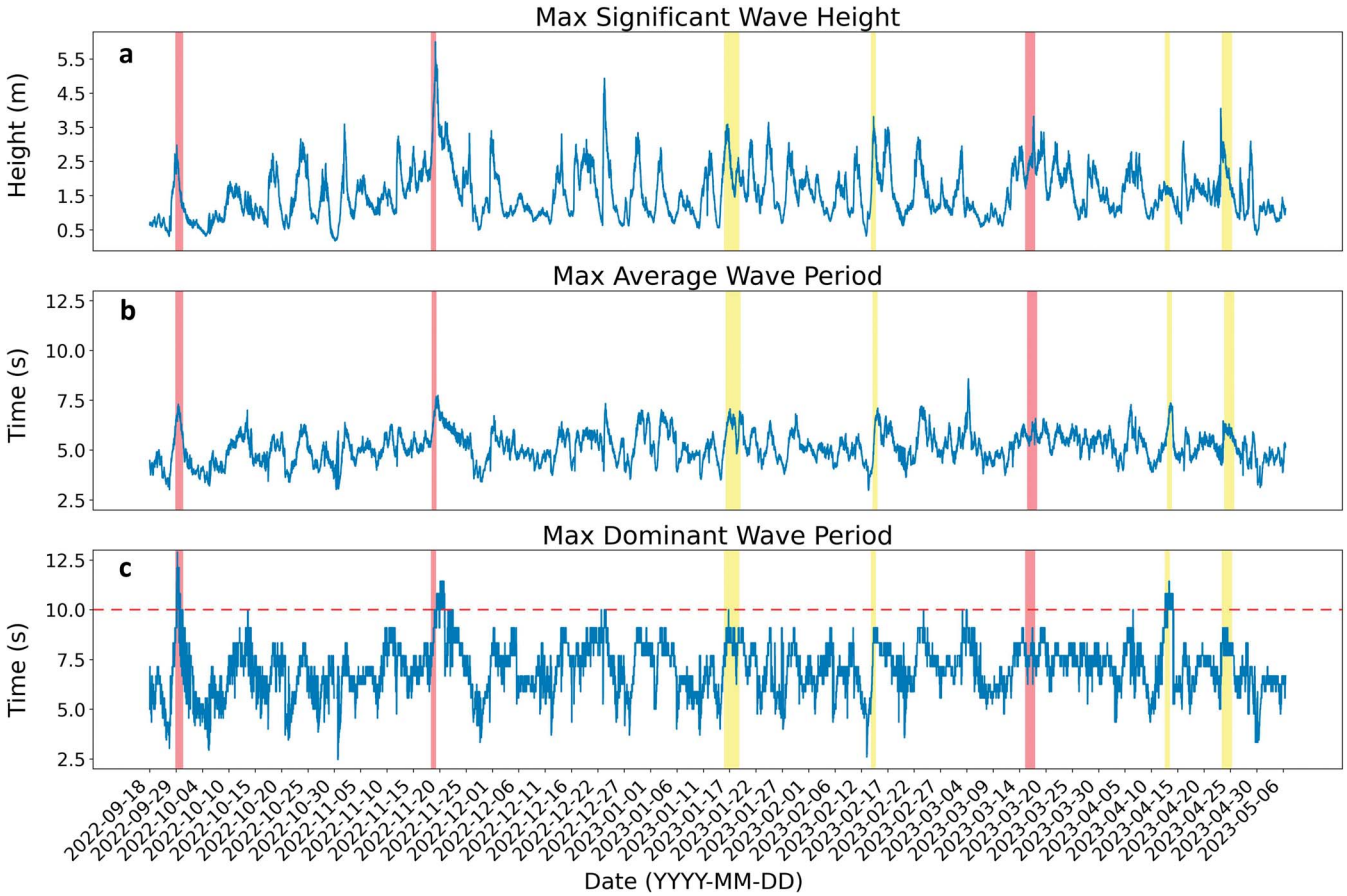

Figure 11. Representation of (a) maximum significant wave height, (b) maximum average wave period, and (c) maximum dominant wave period. The maximum values were obtained after combining NDBC 42019 and NDBC 42020 data. Red columns: full inundation events; yellow columns: partial inundation events.

how changes in offshore wave characteristics and water level influence the dynamics of beach inundation and erosion.

Finally, Figure 7f compares the beach morphologies of the first and the last survey of the study period. Little change is observed over this 13-month interval, suggesting that the recorded erosion events with sand redistribution are followed by more progressive recovery events with an overall seasonally stable berm for this beach. The observations are consistent with previous studies over longer temporal scales conducted by Gibeaut *et al.* (2001), Morton and Pieper (1977), and Williams and Turner (2022).

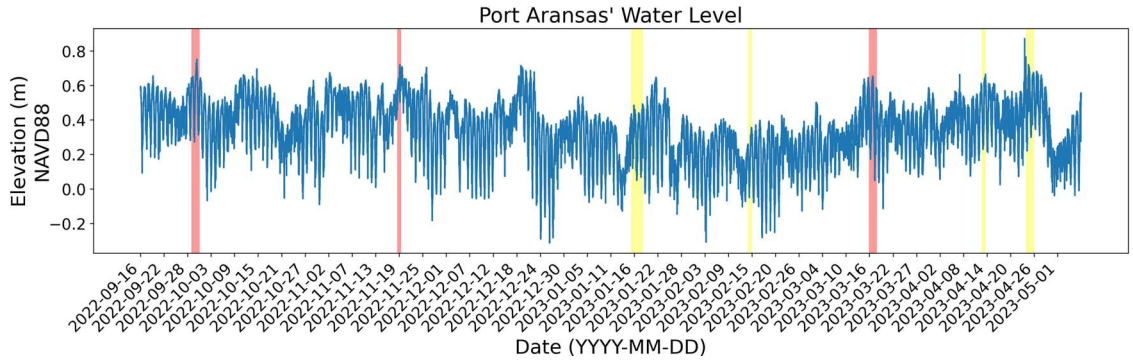

Figure 12. Representation of water-level data (Port Aransas) during inundation events. Red columns: full inundation events; yellow columns: partial inundation events. The width of each column corresponds to the duration of the respective inundation events.

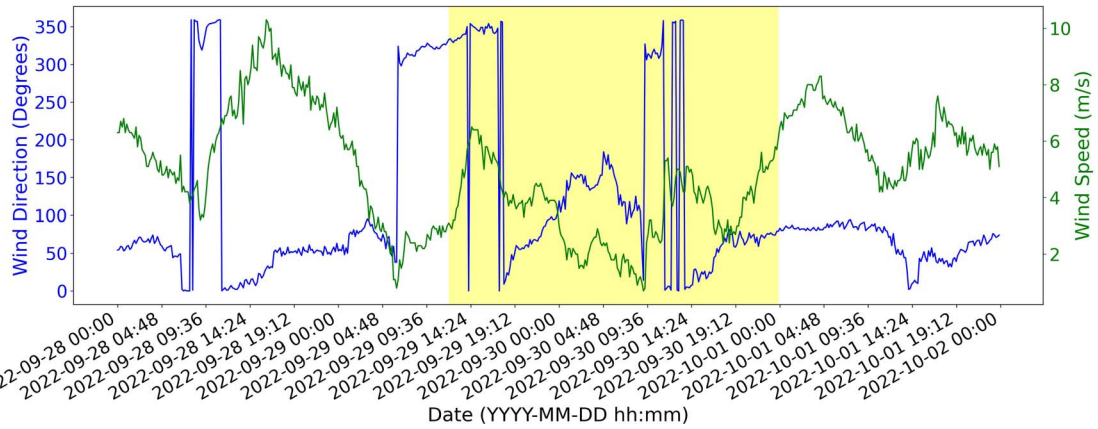

Figure 13. Wind time series for inundation event of 29 September 2022. The yellow band highlights the 4 hours before the image of the beach captured at 1720 and presented in Figure 10.

As discussed in the "Unique Characteristics of the Study Area" subsection, the results of this study are for a very specific beach just south of a long jetty where the berm is wider and the elevation is higher than most of the beach segments farther south along Mustang Island and the northern part of North Padre Island (excluding the beaches near Packery Channel). Therefore, these results of limited periodic inundation are location dependent, and it is anticipated, based on visual observation, that during the study period, these other beaches experienced a higher frequency of coastal inundation, in some cases up to the foredunes.

Comparison of the Wet/Dry Shoreline Elevation with Tidal Datums

Tidal datums are frequently applied in beach management and regulatory processes. The relationship between measured average water level and the respective elevations of tidal datums is not straightforward and can even be misleading for microtidal beaches with strong metocean forcings, such as in the study area. Imagery from pier-mounted cameras was applied to determine the dynamic shifts in the location and elevation of wet/dry shorelines (Vicens-Miquel *et al.*, 2022a; Vicens-Miquel *et al*., 2022b). A systematic process was employed to compute the elevation of the wet/dry shoreline. Initially, the camera imagery was georeferenced using a projective transformation. Sequentially, the wet/dry shoreline was identified and overlaid onto a digital elevation model (DEM). These DEMs were sourced from survey data, with preference given to the most recent survey corresponding to the current imagery. Following the superposition of the imagery, numerous elevation points were extracted. These points were sorted based on their values, eliminating the top and bottom 5% to mitigate the impact of elevation outliers. Subsequently, the mean value of the remaining points was calculated, defining it as the wet/dry shoreline elevation for that specific time of day. Figure 16 details a time series of four wet/dry shoreline elevation measurements per day and compares

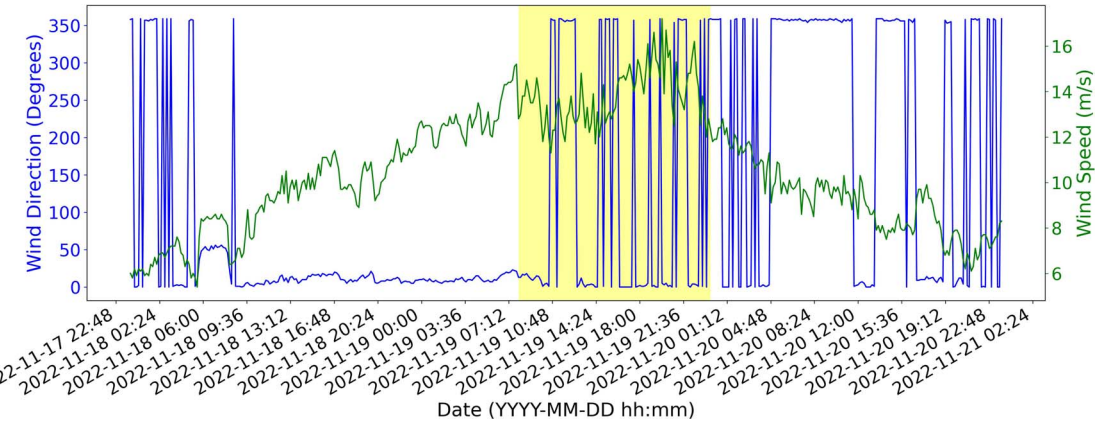

Figure 14. Wind for the second inundation event (19 November 2022). The yellow band highlights the 4 hours before the image of the beach was captured at 1400 (Figure 11).

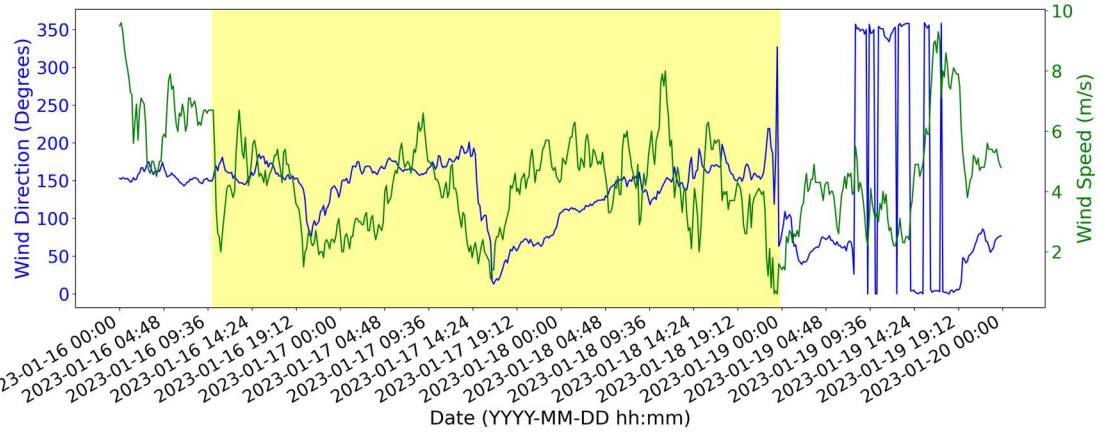

Figure 15. Wind for the second inundation event on 18 January 2023 (1400 [central daylight time]) to match the picture.

it with a time series of average water level measured simultaneously at the nearby Aransas Channel tide gauge.

The average elevation of the wet/dry shoreline during the study was 0.77 m above NAVD88, significantly higher than the average water level recorded at a nearby tide gauge of 0.16 m above NAVD88 for the same period. This location's 0.61 m difference is larger than twice the tidal range; other differences include the seasonality of the respective signals. The average water-level signal displays the expected seasonality with lower levels during the July to August period, increasing water level after that through the end of September, and then water level increasing from February through May (NOAA, 2023c). The time series of the wet/shoreline elevations display only a dampened seasonality, with the variability dominated by individual events, particularly during the first part of the study from February through May 2023. Overall, the relationship between average water level and wet/dryshoreline elevations is not straightforward. This is not surprising because the significant height of nearshore waves is a good predictor of the wave runup (Roberts, Wang, and Kraus, 2010), hence driving the difference between average water level and the elevation of the wet/dry shoreline. Large increases in the wet/dry shoreline elevation can occur, whereas little change occurs in the average water level measured at nearby stations during periods of increasing maximum significant wave height or wave period, as discussed in

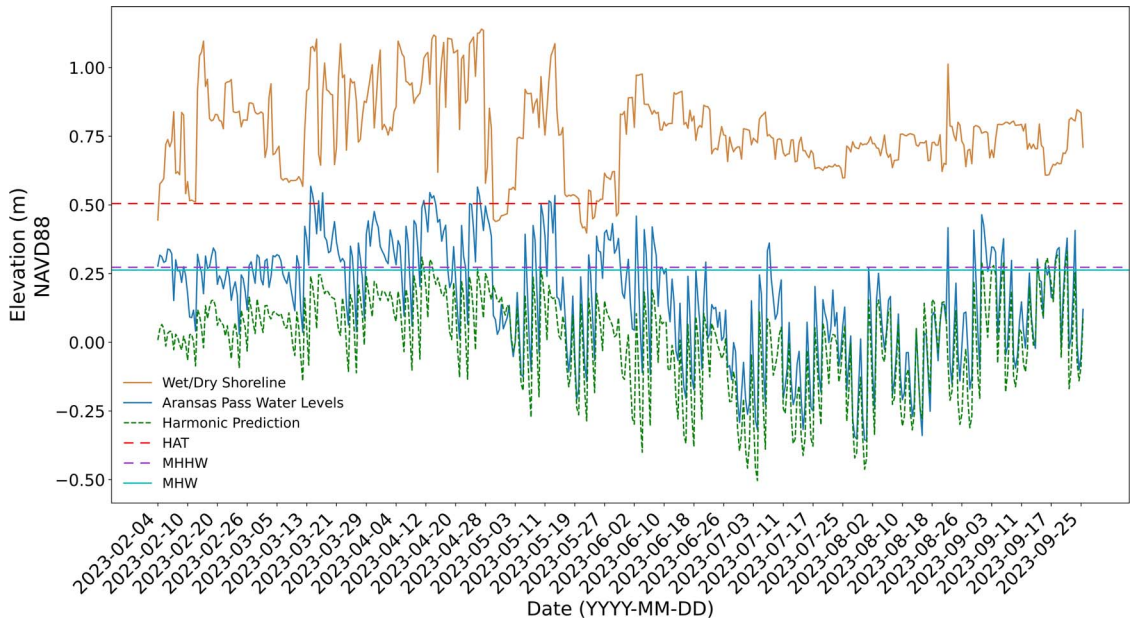

Figure 16. Time series of the wet and dry shoreline elevations (orange) and the average water level (blue) measured at the tide gauge station 8775237, Port Aransas, Texas, compared with frequently used tidal datums relative to the tide gauge station.

the previous section. Because of the absence of real-time nearshore wave measurements along the Texas coast during the study period, wave information came from the aforementioned NDBC deep-water buoys. Although these buoy measurements, particularly wave periods, provide general wave conditions and nearshore winds, onshore or offshore directions will have a significant impact on nearshore maximum significant wave height, making it difficult to perform a more detailed analysis of the relationship between average water level and wet/dry shoreline height.

Some of the limitations of the study include wet/dry shoreline elevations that are measured only during the daytime and weather conditions that will influence the rate at which the wet beach dries and, hence, the latency of the location of the wet/dry shoreline. The absence of nighttime observation is somewhat mitigated by checking the early morning imagery and looking at other metocean recorded observations that may suggest the possibility of a coastal inundation during the night.

Figure 16 compares the measurements of both the average water level and the wet/shoreline elevation to the commonly applied tidal datums (*i.e.* MHW, MHHW, HAT) for the nearby tide gauge 8775237, Port Aransas, Texas. The comparisons show that the average water level measured at nearby monitoring stations regularly exceeds the MHW and MHHW tidal datums but rarely the HAT datums. It is critical for beach stakeholders to understand that the MHW and MHHW elevations are not indicative of a particularly high-water level for this location and the Texas coast in general. The higher elevation HAT datum is a better indication of the highest average water level reached, without accounting for wave runup, for locations such as the study area given the local metocean forcings. When possible, it is recommended to use the HAT line as a survey reference level for beach management purposes because it is a better indication of a high-water mark for the location and will be more practical to survey, leading to more accurate measurements because the berm at MHHW is frequently inundated.

Figure 16 further shows that the wet/dryshoreline always exceeds the MHHW datum and predominantly exceeds the HAT datum. Beach managers should be aware of these comparisons when using these different tidal datums for typical beach management and planning. These differences also emphasize that for this location and other beaches with similar metocean characteristics, it is vital to have a more comprehensive suite of parameters applied in measurements and models rather than just water level or surge models to predict potential beach inundation.

CONCLUSIONS

The study of a small representative segment of the beach adjacent to Horace Caldwell Pier at I.B. Magee Beach Park, Port Aransas, Texas, has provided valuable insights into the intricate dynamics of beach morphology over short temporal periods. Throughout the year-long investigation, relatively significant changes in the area between successively surveyed beach profiles were associated with increased wave energy, in particular dominant wave period longer than 10 seconds. This phenomenon underscores the direct influence of wave and water-level dynamics on beach morphology, with higher energy events leading to erosion across beach profiles that result in significant changes in the beach morphology. Specific metocean conditions accompany these morphological changes as well as inundation events that reach further landward than common water level forecasting tools predict.

The investigation differentiated between two distinct types of inundation events: one that does not cause erosion and a second type that leads to erosion along the focused beach segment. An increase in maximum significant wave height, maximum average dominant wave period, and average water level initiated both types of events. In the first scenario, where erosion does not occur, no large increases occurred in the maximum dominant wave period. In cases of beach erosion, a substantial increase in the offshore maximum dominant wave period was measured with a threshold for beach erosion in the study cases at approximately 10 seconds. Consequently, whether an increase in the maximum dominant wave period occurs or not may be the determining factor for beach erosion in the study area, whereas increases in nearshore winds did not have a direct influence on the beach inundation and erosion cases of the study. This differentiation underscores the pivotal role that wave energy, particularly the dominant maximum wave period, plays in influencing the erosive impact of inundation events. A comprehensive understanding of these event-specific triggers and outcomes is necessary for an accurate prediction that supports effective proactive management of potential beach erosion scenarios.

Seven partial or full inundation events were recorded (real-time continuous video) over the 13 months' investigation, indicating that such events were not frequent in the Port Aransas area. This infrequency can be justified by considering the local climatic and oceanographic conditions in addition to the wide berm width and higher elevation that this beach segment has in comparison with the majority of the coastline along Mustang and North Padre Island. The relatively low occurrence of inundation events in this area underscores the value of recognizing the specific context of each coastal region when formulating management strategies. Although this study provides valuable insights into the dynamics of beach morphology and inundation events on the north end of Mustang Island, the study was relatively short, with 13 months of survey data and imagery. Longer time series are necessary to strengthen the conclusions and refine the inundation and erosion thresholds; hence, continued research and monitoring are underway and are crucial for further refining predictive models. Such models enhance the understanding of these complex coastal processes, particularly for application along narrower, low-elevation beach segments that dominate the coastline.

The time series of total water levels, including wave runup, were compared with observed average water levels and tidal datums at a colocated tide gauge, as well as the related tidal datums frequently used for beach studies and management. The comparison concluded that the total water levels were on average 0.6 m above the average water levels. Furthermore, the water levels were above the HAT datum for most of the 13 months' study period and always above the MHW and MHHW datums. Although generally below the wet/dry shoreline elevation, the higher elevation HAT tidal datum was

mostly above the average water levels for this location. These results show that beach management and operations could benefit from using HAT datum rather than the MHW, which is commonly used, as a better suited indicator of high water levels for this and nearby beaches and for surveys defining limits of inundation and decision-making.

Future work in this research involves developing an operational real-time inundation model specifically designed for the studied area. This research is essential because it enables a nuanced understanding of beach changes and their correlation with metocean conditions. It serves as a foundational step toward developing an accurate real-time inundation model that focuses on parameters of significance, such as the maximum dominant wave period. Thus, this research holds significant value for beach managers and stakeholders, serving as an essential component of the ongoing inundation model development.

ACKNOWLEDGMENTS

This material is based upon work supported by the National Science Foundation under Grant No. RISE-2019758 within the NSF AI Institute for Research on Trustworthy AI in Weather, Climate, and Coastal Oceanography (AI2ES). Any opinions, findings, and conclusions or recommendations expressed in this material are those of the author(s) and do not necessarily reflect the views of the National Science Foundation.

The authors acknowledge the efforts of the survey team (Judy Millien, Yasmin Himsieh, Wyatt Miller, and Spencer Berglund), the data collection team (Matthew Kastl, Savannah Stephenson, and Beto Estrada), and Katie Colburn in support of this research. The support of Scott Cross with the Nueces County Parks System is also acknowledged for hosting the instrument ensemble on Horace Caldwell Pier which made this research possible.

LITERATURE CITED

Bernabeu Tello, A.M.; Medina Santamaría, R., and Vidal Pascual, C., 2002. An equilibrium profile model for tidal environments. *Scientia Marina*, 66(4), 325–335.

Carrasco, A.R.; Ferreira, O.; Matias, A.; Pacheco, A., and Freire, P., 2011. Short-term sediment transport at a backbarrier beach. *Journal of Coastal Research*, 27(6), 1076–1084.

Coco, G.; Burnet, T.K.; Werner, B., and Elgar, S., 2004. The role of tides in beach cusp development. *Journal of Geophysical Research: Oceans*, 109(C4).

Fabiyi, O. and Yesuf, G., 2016. Dynamics and characterization of coastal flooding in Nigeria: Implication for local community management strategies. *Life Research Publications in Geography*, 12(1), 45–61.

Fox, W.P. and Davis, R.A., 1978. Seasonal variation in beach erosion and sedimentation on the Oregon coast. *Geological Society of America Bulletin*, 89(10), 1541–1549. doi:10.1130/0016-7606(1978)89<1541:SVIBEA>2.0.CO;2

Garel, E.; Sousa, C., and Ferreira, O., 2015. Sand bypass and updrift beach evolution after jetty construction at an ebb-tidal delta. *Estuarine Coastal and Shelf Science*, 167(part A), 4–13. doi:10.1016/j.ecss.2015.05.044

Gibeaut, J.C.; Hepner, T.; Waldinger, R.L.; Andrews, J.R.; Gutierrez, R.; Tremblay, T.A., and Smyth, R.C., 2001. *Changes in Gulf Shoreline Position, Mustang and North Padre Islands, Texas*. Austin, Texas: The University of Texas at Austin, Bureau of Economic Geology, *Report of the Texas Coastal Coordination Council Pursuant to National Oceanic and Atmospheric Administration Award No. NA97OZ0179*. GLO Contract Number 00-002R.

Gillie, R.D., 1997. Causes of coastal erosion in Pacific Island nations. *Journal of Coastal Research*, 24, pp. 173–204.

Gordon, A.D. and Nielsen, L., 2020. Large scale impacts of jetties and training walls-experience on the Australian east coast. *Coastal Engineering Proceedings*. doi:10.9753/icce.v36v.structures.2

Hague, B.S. and Taylor, A.J., 2021. Tide-only inundation: A metric to quantify the contribution of tides to coastal inundation under sea-level rise. *Natural Hazards*, 107(1), 675–695.

Hamilton, D.G.; Ebersole, B.A.; Smith, E.R., and Wang, P., 2001. *Development of a Large-Scale Laboratory Facility for Sediment Transport Research*. Washington, DC: U.S. Army Corps of Engineers, Final Report, 160 p.

Hunter, R.E.; Richmond, B.M., and Alpha, T.R., 1983. Storm-controlled oblique dunes of the Oregon coast. *Geological Society of America Bulletin*, 94(12), 1450–1465. doi:10.1130/0016-7606(1983)94<1450:SODOTO>2.0.CO;2

Jackson, D.; Cooper, J., and dDel Rio, L., 2005. Geological control of beach morphodynamic state. *Marine Geology*, 216(4), 297–314.

Jeon, H.; Eem, S.-H., and Park, J., 2018. Flood damage assessment in building scale caused by the coastal inundation height at Haeundae Beach, Busan. *In:* Shim, J.-S.; Chun, I. and Lim, H.S. (eds.), *Proceedings from the International Coastal Symposium (ICS) 2018* (Busan, Republic of Korea). *Journal of Coastal Research*, Special Issue No. 85, pp. 1561–1565.

Knezek, E.B., 1997. Equilibrium Beach Profile Measurement and Sediment Analysis: Mustang Island, Texas. Monterey, California: Naval Postgraduate School, Ph.D. dissertation, 169 p. https://core.ac.uk/download/pdf/36701871.pdf

Knight, J. and Burningham, H., 2003. Recent ventifact development on the central Oregon coast, western USA. *Earth Surface Processes and Landforms*, 28(1), 87–98. doi:10.1002/esp.432

Krestenitis, Y.N.; Androulidakis, Y.S.; Kontos, Y.N., and Georgakopoulos, G., 2011. Coastal inundation in the north-eastern Mediterranean coastal zone due to storm surge events. *Journal of Coastal Conservation*, 15, 353–368.

Ludka, B.C.; Guza, R.T.; O'Reilly, W.C., and Yates, M., 2015. Field evidence of beach profile evolution toward equilibrium. *Journal of Geophysical Research: Oceans*, 120(11), 7574–7597. doi:10.1002/2015JC010893

Masselink, G.; Kroon, A., and Davidson-Arnott, R., 2006. Morphodynamics of intertidal bars in wave-dominated coastal settings—A review. *Geomorphology*, 73(1–2), 33–49.

Mcinnes, K.L., Walsh, K.J.E., Hubbert, G.D., & Beer, T., 2003. Impact of sea-level rise and storm surges on a coastal community. *Natural Hazards*, 30, 187–207.

Miller, J.K. and Dean, R.G., 2004. A simple new shoreline change model. *Coastal Engineering*, 51(7), 531–556. doi:10.1016/j.coastaleng.2004.05.006

Morton, R.A. and Pieper, M.J., 1977. *Shoreline Changes on Mustang Island and North Padre Island (Aransas Pass to Yarborough Pass): An Analysis of Historical Changes of the Texas Gulf Shoreline*. Austin, Texas: The University of Texas at Austin, Bureau of Economic Geology, *Geological Circular*, 77-1, 45.

Moser, S.C.; Jeffress Williams, S., and Boesch, D.F., 2012. Wicked challenges at land's end: Managing coastal vulnerability under climate change. *Annual Review of Environment and Resources*, 37, 51–78.

National Oceanic and Atmospheric Administration (NOAA), 2023a. *Find your local tides and currents: Texas*. https://tidesandcurrents.noaa.gov/map/index.html?region=Texas

NOAA, 2023b. *Relative sea level trend 8771341 Galveston Bay entrance, Texas*. https://tidesandcurrents.noaa.gov/sltrends/sltrends_station.shtml?id=8771341

NOAA, 2023c. *Relative sea level trend 8775870 Corpus Christi, Texas*. https://tidesandcurrents.noaa.gov/sltrends/sltrends_station.shtml?id=8775870

NOAA, 2023d. *Station 42019*. https://www.ndbc.noaa.gov/station_page.php?station=42019

NOAA, 2023e. *Station 42020*. https://www.ndbc.noaa.gov/station_page.php?station=42020

NOAA, 2023f. *Station PTAT2 - Port Aransas, TX*. https://www.ndbc.noaa.gov/station_page.php?station=ptat2

NOAA, 2023g. *Tide predictions: 8775241, Aransas, Aransas Pass, TX*. https://tidesandcurrents.noaa.gov/noaatidepredictions.html?id=8775241&legacy=1

Oregon State University, 2023. *O.H. Hinsdale Wave Research Laboratory*. https://engineering.oregonstate.edu/wave-lab

Pacheco, A.; Horta, J.; Loureiro, C., and Ferreira, O., 2015. Retrieval of nearshore bathymetry from Landsat 8 images: A tool for coastal monitoring in shallow waters. *Remote Sensing of Environment*, 159, 102–116.

Pianca, C.; Holman, R.A., and Siegle, E., 2015. Shoreline variability from days to decades: Results of long-term video imaging. *Journal of Geophysical Research: Oceans*, 120(3), 2159–2178. doi:10.1002/2014JC010329

Plant, N.G.; Holman, R.A.; Freilich, M.H., and Birkemeier, W.A., 1999. A simple model for interannual sandbar behavior. *Journal of Geophysical Research: Oceans*, 104(C7), 15755–15776. doi:10.1029/1999JC900112

Pollard, J.; Spencer, T., and Brooks, S., 2019. The interactive relationship between coastal erosion and flood risk. *Progress in Physical Geography: Earth and Environment*, 43(4), 574–585.

Prasad, D.H. and Kumar, N.D., 2014. Coastal erosion studies—A review. *International Journal of Geosciences*, 5(3). doi:10.4236/ijg.2014.53033

Prasetya, G., 2007. Chapter 4: Protection from coastal erosion. Thematic paper: The role of coastal forests and trees in protecting against coastal erosion. *Rapid Appraisal Procedure Publication (FAO)*. https://www.fao.org/4/ag127e/ag127e09.htm

Roberts, T.M.; Wang, P., and Kraus, N.C., 2010. Limits of wave runup and corresponding beach-profile change from large-scale laboratory data. *Journal of Coastal Research*, 26(1), 184–198.

Saadon, M.S.I.; Ab Wahida, N.S.; Othman, M.R.; Nor, D.A.M.; Mokhtar, F.S.; Nordin, N.; Kowang, T.O., and Nordin, L., 2020. An evaluation of the impact of coastal erosion to the environment and economic activities at Mengabang Telipot, Terengganu. *Journal of Critical Reviews*, 7(8), 1132–1136.

Splinter, K.D.; Turner, I.L.; Davidson, M.A.; Barnard, P.; Castelle, B., and Oltman-Shay, J., 2014. A generalized equilibrium model for predicting daily to interannual shoreline response. *Journal of Geophysical Research: Earth Surface*, 119(9), 1936–1958.

Suanez, S.; Cancouët, R.; Floc'h, F.; Blaise, E.; Ardhuin, F.; Filipot, J.-F.; Cariolet, J.-M., and Delacourt, C., 2015. Observations and predictions of wave runup, extreme water levels, and medium-term dune erosion during storm conditions. *Journal of Marine Science and Engineering*, 3(3), 674–698. doi:10.3390/jmse3030674

Texas Natural Resources Code, 2024. *Natural resources code: Beaches and dunes: Use and maintenance of public beaches: General provisions: Section 61.012*. https://statutes.capitol.texas.gov/Docs/NR/htm/NR.61.htm

U.S. Army Corps of Engineers (USACE), 2023a. *Engineer research and development center website*. https://www.erdc.usace.army.mil/

USACE, 2023b. WIS data portal. https://wisportal.erdc.dren.mil/

van Rijn, L., 2011. Coastal erosion and control. *Ocean & Coastal Management*, 54(12), 867–887.

Vicens-Miquel, M.; Medrano, F.A.; Tissot, P.; Kamangir, H., and Starek, M., 2022a. Deep learning automatic detection of the wet/dry shoreline at fish pass, Texas. *IGARSS 2022-2022 IEEE International Geoscience and Remote Sensing Symposium*, Kuala Lumpur, Malaysia, 1876–1879. doi:10.1109/IGARSS46834.2022.9884633

Vicens-Miquel, M.; Medrano, F.A.; Tissot, P.E.; Kamangir, H.; Starek, M.J., and Colburn, K., 2022b. A deep learning based method to delineate the wet/dry shoreline and compute its elevation using high-resolution UAS imagery. *Remote Sensing*, 14(23), 5990.

Wang, X.; Xu, L.-L.; Cui, S.-H., and Wang, C.-H., 2020. Reflections on coastal inundation, climate change impact, and adaptation in built environment: Progresses and constraints. *Advances in Climate Change Research*, 11(4), 317–331.

Williams, D.D. and Turner, R.L., 2022. *Nueces County Beach and Coastal Resource Monitoring Program: Post-2020 Hurricane Season Assessment of Gulf Coast Beaches and Baseline Establishment*. *Technical Report for Nueces County Coastal Parks Department*, 36 p.